DOI: 10.1002/ejic.201001259

Green Wet Chemical Route for the Synthesis of Silver and Palladium Dendrites

Bineta Keita,*[a] L. R. Brudna Holzle,[a,b] Rosa Ngo Biboum,[a] Louis Nadjo,[a] Israel M. Mbomekalle,[c] Sylvain Franger,[d] Patrick Berthet,[d] François Brisset,[e] Frederic Miserque,[f] and Georges A. Ekedi[a]

Keywords: Nanoparticles / Nanostructures / Dendrites / Silver / Palladium

A novel and very effective wet chemical route for the preparation of metal dendritic nanostructures was developed by starting from $VOSO_4$ and Ag_2SO_4 (or K_2PdCl_4) in aqueous solution at room temperature. No template or surfactant was used. $VOSO_4$ serves as the reducing agent for the silver salt, and the resulting silver nanoparticles and nanocrystallites are then arranged into dendritic structures. The morphologies of the dendrites are found to be heavily influenced both by the molar ratio and the concentrations of the reactants. Observation of symmetric and asymmetric dendrites with variations of these parameters supports the proposal that diffusion and oriented attachment of silver nanoparticles or crystallites might compete, to various extents, and dictate the final morphologies of dendritic nanostructures. To the best of our knowledge, this is the first example of a surfactant-free, template-free, fully inorganic wet chemical route to metal dendritic structures. The method was also successful in the preparation of palladium nanodendrites.

Introduction

The more attractive electrocatalysts currently in use for redox processes are based on metal nanostructures. The major challenge remains the development of efficient, stable, cheap, and environmentally friendly materials. Dendritic architectures have been recognized in several reports to fulfil most of the requirements for exhibiting enhanced properties relative to both discrete nanoparticles and bulk powders. Applications of such structures in the catalysis and technology fields are gaining widespread importance.[1–3] In most cases, the electrochemical method is used for the synthesis of metal dendritic structures. Concentrating specifically on the case of Ag, template- and surfactant-free synthesis of Ag nanodendrites by Yang et al. was performed with use of a suspension of zinc microparticles as a heterogeneous reducing agent.[4] As a truly wet chemical route, a novel preparation of snowflake-like dendritic nanostructures of Ag or Au at room temperature was proposed with *p*-phenylenediamine[5] or dendritic Ag with ascorbic acid,[6] provided the organic reducing agent was in large excess. Finally, dendritic silver synthesis by a surfactant-free, mixed-solvent water–acetone route by using L-ascorbic acid was recently published.[7] Examples of wet chemical routes for the synthesis of dendritic Pd nanostructures are even more scarce.[8,9]

We now report on silver and palladium dendrites generated by a simple wet chemical route using only $VOSO_4$ in water at room temperature, without any template or surfactant. One of us (B. K.) described this method recently in a patent.[10] In the global search for platinum-free catalysts, silver and palladium could be good candidates, provided one can elaborate judicious nanostructures in order to improve their efficiencies. Despite extensive previous use of oxides and polyoxometalates (POMs) for the generation of metal nano-objects,[11] the present report constitutes the first example of surfactant-free, template-free, fully inorganic wet chemical route to dendritic structures.

Results and Discussion

The precursor salts were Ag_2SO_4 and $VOSO_4$. In a typical experiment for Ag dendrite synthesis, a mixture containing 2 mM Ag_2SO_4 (4 mM Ag^+) and 4 mM $VOSO_4$ was as-

[a] Groupe d'Electrochimie et de Photoélectrochimie, Laboratoire de Chimie Physique, UMR 8000, CNRS, Université Paris-Sud XI,
Bâtiment 350, 91405 Orsay Cedex, France
E-mail: bineta.keita@u-psud.fr
[b] Universidade Federal do Pampa, Campus de Bagé,
Rua Carlos Barbosa, s/n°, Getúlio Vargas Bagé – RS, CEP 96412-420, Brazil
[c] Institut Lavoisier, UMR 8180, CNRS, Université de Versailles Saint-Quentin,
45, avenue des Etats-Unis, 78035 Versailles Cedex, France
[d] Laboratoire de Physico-chimie de l'Etat Solide, ICMMO, UMR 8182, CNRS, Université Paris-Sud XI,
Bâtiment 410, 91405 Orsay Cedex, France
[e] ICMMO, UMR 8182 CNRS, Université Paris-Sud XI,
91405 Orsay Cedex, France
[f] Commissariat à l'Energie Atomique (Saclay)/Département de Physico-Chimie/Laboratoire Réactivité des Surfaces et Interfaces,
Bâtiment 391, 91191 Gif-sur-Yvette cedex, France
Supporting information for this article is available on the WWW under http://dx.doi.org/10.1002/ejic.201001259.

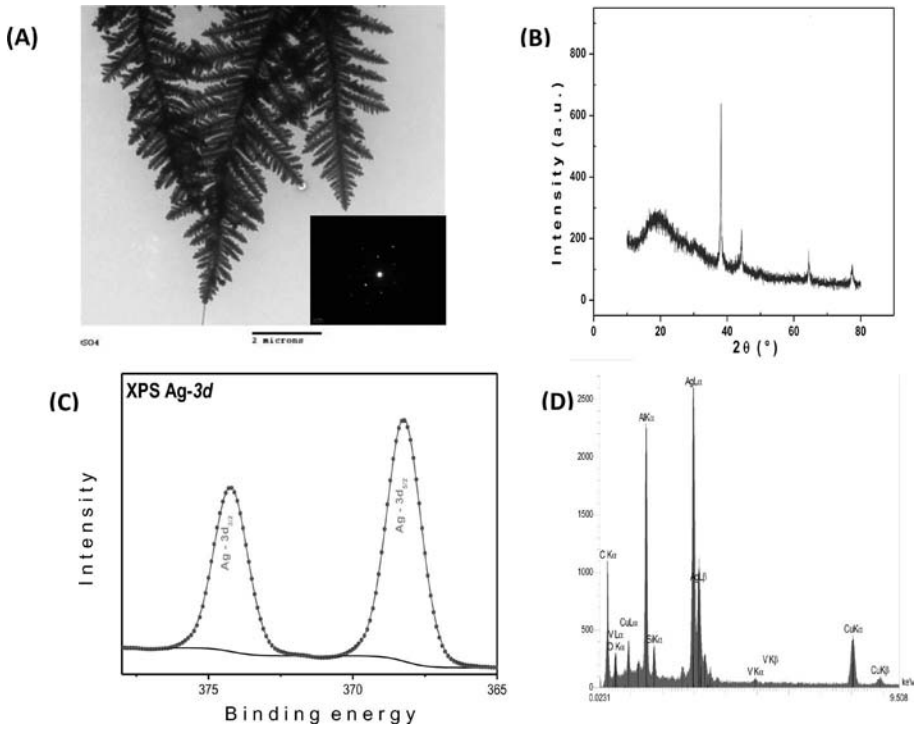

Figure 1. (A) Low-magnification TEM image of a typical symmetric silver dendrite obtained for $\gamma = 1$ and $C^0_{Ag+} = 4.0$ mM; (B) XRD pattern of as-synthesized silver nanodendrites; (C) deconvolution of the silver core 3d level XPS spectrum; (D) EDS microanalysis of the dendrites.

sembled in Millipore water and kept at room temperature. The excess parameter is defined as $\gamma = [Ag^+]/[VOSO_4]$. The color of the solution changed rapidly, and a large amount of precipitate gradually formed. The solid was collected by centrifugation, thoroughly washed several times with water, and finally re-dispersed in water for characterization. A representative low-magnification TEM image of a typical dendritic nanostructure is shown in Figure 1A for C^0_{Ag+} = 4 mM and $\gamma = 1$. The dendrite appears as a remarkably hierarchical structure constituted by several generations with apparent self-similarity. An overall high symmetry is observed, with angles between the stem and branches uniformly in the range 50°–60°. Branches at the tip of the stem are shorter than those at its base, thus creating a tree-like structure. The selected area electron diffraction (SAED) spectra recorded at several positions, including stem and branches, exhibit a typical hexagonal symmetry (that in the inset of Figure 1A indicates that the dendrite is a single crystal; see also Figure S1, obtained from a whole branch). The XRD diffraction peaks collected in the range $10° < 2\theta < 80°$ at $2\theta = 38.14$, 44.35, 64.47, and 77.47 (Figure 1B) can be indexed to the (111), (200), (220), and (311) reflections of the cubic Ag, respectively. The intensity ratio between the (111) and the (220) XRD diffraction peaks is higher than that of the standard file (JCPDS 04–0783) (5.7 vs. 2.5), which confirms that the dendrites grow with a preferred orientation [large fraction of (111) facets]. No vanadium oxide was detected in this diffraction spectrum. The XPS spectrum in the Ag-$3d_{5/2}$ and Ag-$3d_{3/2}$ binding energy region shows peaks centered at 368.2 ± 0.3 and 374.2 ± 0.3 eV, respectively, indicating that metallic silver was deposited (Figure 1C). X-ray energy dispersive spectroscopy (EDS) microanalysis (Figure 1D) shows only the Ag peak at about 3 eV. The other peaks in this spectrum can be assigned to Cu from the Cu grid, C from holey carbon on the grid, in particular, Al and Si coming from the sample holder (STEM detector). It is worth noting that the amount of vanadium is negligibly small. In summary, pure Ag metal nanodendrites are obtained. Detection of vanadium in XPS spectra in the as-prepared mixtures is discussed and rationalized in the Supporting Information in conjunction with XRD and EDS analyses (Figure S2).

Depending on the initial concentrations of reactants, different silver nanostructures are observed (see Figure 2 and the accompanying Figure S3). In Figure 2, the value $\gamma = 1$ was kept throughout. With $C^0_{Ag+} = 0.25$ mM, a representative TEM image in Figure 2A shows long nanowires. Another domain shows that these nanowires are actually surrounded by an abundance of nanoparticles (Figure S3A). Also, Figure 2B includes some nanowires with very short branches prefiguring dendritic structures. Finally, starting from values of $C^0_{Ag+} = 1.0$ mM and higher, dendrites become by far the dominant morphological structures with two simultaneously observed main variants: symmetrical dendrites (Figures 1A and 2C) and asymmetrical ones (Figure 2D) observed for all concentrations $C^0_{Ag+} \geq 1.0$ mM. Asymmetrical dendritic structures appear dense, with fewer straight stems and branches. The angles between stems and branches are rather random, giving the appearance of a disordered structure (see Figures S3C and S3D). In addition,

Figure S3D highlights the presence of an environment of organized nanostructures, which seem to consist of vanadium oxide, containing Ag nanoparticles (see also Figure S2). Future work will try to elucidate the very nature of this environment. No significant new feature was observed for other combinations of γ and C^0_{Ag+}.

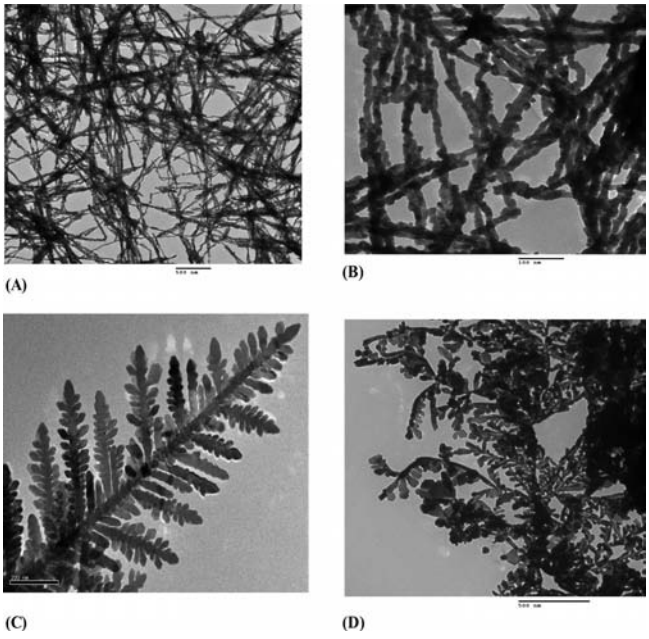

Figure 2. (A) Low-magnification TEM image of the centrifuged and washed Ag^0 nanowires (γ = 1 and C^0_{Ag+} = 0.25 mM); (B) high-magnification TEM image of the centrifuged and washed Ag^0 nanowires (γ = 1 and C^0_{Ag+} = 0.25 mM); (C) new representative low-magnification TEM image of a typical symmetric silver dendrite obtained for γ = 1 and C^0_{Ag+} = 4.0 mM; (D) TEM image of a typical asymmetric silver dendrite obtained for γ = 1 and C^0_{Ag+} = 10.0 mM.

Various models are useful to analyze fractal phenomena,[12] including the deposition–diffusion aggregation model, the diffusion-limited aggregation (DLA) model, and the cluster–cluster aggregation model. Possible mechanistic pathways for the formation of symmetrical and asymmetrical dendrites are developed in the Supporting Information.

The same approach was applied to a mixture of K_2PdCl_4 and $VOSO_4$ with γ = 1. Figure 3 shows representative dendritic features observed at a low palladium concentration. Further details are presented in the Supporting Information. Figure 3B shows a representative magnified image of the blackberry-like dendritic structure obtained for C^0_{Pd2+} = 0.25 mM with a diameter around 185 nm. The same dendritic structure was observed with higher concentrations (Figure S4). However, its size and dispersity depend on the initial concentration. XRD spectra for several initial concentrations of reactants (Figure S4C) indicate the good crystallinity of the Pd deposits.

Indeed, the difference in morphology between Ag and Pd nanodendrites obtained by using the present wet chemical route is worth pointing out. First, we must recall that most dendritic structures are synthesized by electrochemical deposition[13] and that wet chemical routes are more

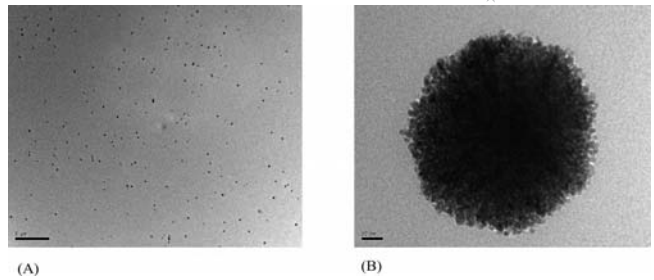

Figure 3. TEM images of typical Pd^0 dendritic structures obtained for γ = 1 and C^0_{Ag+} = 0.25 mM: (A) very low magnification; (B) high magnification.

scarce.[4–9] Second, whatever the method, the observed final morphology of the nanodendrites depends on several parameters, including the extent of adsorption or complexation among reactants, the working electrode potential in electrochemistry, and the injection sequence of reactants and eventual surfactants in wet chemical routes. In the present example of palladium nanodendrites, it is likely that the observed morphology, as also described in the literature,[9] must be ascribed to the interplay of such parameters, resulting in the modulation of the reduction kinetics at the early stages of the reaction.

Conclusions

The present observations support the assumption that the simple use of $VOSO_4$ as reducing agent, in water, at room temperature, is a general method for the preparation of dendritic Ag and Pd nanostructures from Ag_2SO_4 and K_2PdCl_4, respectively. To the best of our knowledge, this is the first use of $VOSO_4$ as reducing agent for the synthesis of dendritic metal nanostructures. The method might constitute a general wet chemical route for the fabrication of noble metal nanodendrites, including Ag and Pd, and will be extended to other metals. Future work will explore the properties of these structures, including electrocatalytic applications.

Supporting Information (see footnote on the first page of this article): Experimental conditions, mechanisms of dendrite formation, additional TEM images with X-ray diffraction, XPS, XRD and EDS analyses.

Acknowledgments

Financial support from the Centre National de la Recherche Scientifique (UMR 8000, UMR8180 and 8182), Université Paris-Sud 11 and Université de Versailles are gratefully acknowledged.

[1] M. H. Ullah, W.-S. Chung, I. Kim, C.-S. Ha, *Small* **2006**, *2*, 870–873.
[2] K. Yamada, K. Miyazaki, S. Koji, Y. Okumura, M. Shibata, *J. Power Sources* **2008**, *180*, 181–184.
[3] See for example: a) H. Yan, R. He, J. Johnson, M. Law, R. J. Saykally, P. Yang, *J. Am. Chem. Soc.* **2003**, *125*, 4728–4729; b) C. D. Geddes, A. Parfenov, I. Gryczynski, J. R. Lakowicz, *J. Phys. Chem. B* **2003**, *107*, 9989–9993; c) C. Kim, H. Lee, *Catal.*

Commun. **2009**, *11*, 7–10; d) Z.-H. Lin, M.-H. Lin, H.-T. Chang, *Chem. Eur. J.* **2009**, *15*, 4656–4662.
[4] X. Wen, Y.-T. Xie, M. W. C. Mak, K. Y. Cheung, X.-Y. Li, R. Renneberg, S. Yang, *Langmuir* **2006**, *22*, 4836–42.
[5] X. Sun, M. Hagner, *Langmuir* **2007**, *23*, 9147–950.
[6] G. A. Martínez-Castañón, N. Niño-Martínez, J. P. Loyola-Rodríguez, N. Patiño-Marín, J. R. Martínez-Mendoza, F. Ruiz, *Mater. Lett.* **2009**, *63*, 1266–1268.
[7] Y. Han, S. Liu, M. Han, J. Bao, Z. Dai, *Cryst. Growth Des.* **2009**, *9*, 3941–3947.
[8] Ishama Naoki Jpn. Kokai Tokkyo Koho CODEN: JKXXAF JP 07149524 A 19950613 Heisei Application: JP 93-299624 19931130; priority: CAN 123:174289 AN 1995:759313, **1995**, 4 pp.
[9] Y. W. Lee, M. Kim, S. W. Han, *Chem. Commun.* **2010**, *46*, 1535–1537.
[10] B. Keita, Fr. Demande, Centre National de la Recherche Scientifique (C.N.R.S.), FR2937978 A1 20100507, **2010**.
[11] R. N. Biboum, B. Keita, S. Franger, C. P. Nanseu Njiki, G. Zhang, J. Zhang, T. Liu, I. M. Mbomekallé, L. Nadjo, *Materials* **2010**, *3*, 741–754 and references cited therein.
[12] see for example: a) T. A. Witten Jr., L. M. Sander, *Phys. Rev. Lett.* **1981**, *47*, 1400–1403; b) B. Jacob, P. Garik, *Nature* **1990**, *343*, 523–530; c) M. Kolb, R. Botet, R. Jullien, *Phys. Rev. Lett.* **1981**, *51*, 1123–1126.
[13] See for example: a) C. Gu, T.-Y. Zhang, *Langmuir* **2008**, *24*, 12010–12016; b) A. Q. Mohanty, N. Garg, R. Jin, *Angew. Chem. Int. Ed.* **2010**, *49*, 4962–4966; c) J. Yu, T. Fujita, A. Inoue, T. Sakurai, M. Chen, *Nanotechnology* **2010**, *21*, 085601.
Received: December 2, 2010
Published Online: February 3, 2011

